# Development of a new fourth-order hydrodynamic code for Astrophysics


Annop Wongwathanarat

Hannes Grimm-Strele

Ewald Müller


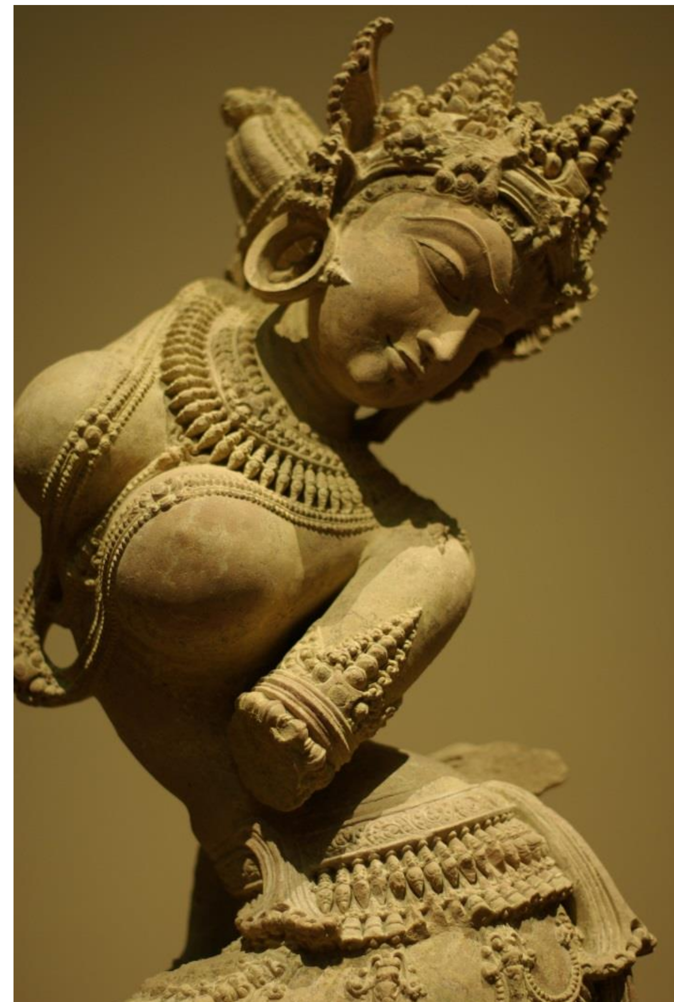

CoCoNuT Meeting 2017


Max-Planck-Institut
für Astrophysik

# Motivation

# Euler equations

$$\frac{\partial \mathbf{U}}{\partial t} + \frac{\partial \mathbf{F}(\mathbf{U})}{\partial x} + \frac{\partial \mathbf{G}(\mathbf{U})}{\partial y} + \frac{\partial \mathbf{H}(\mathbf{U})}{\partial z} = 0$$

Differential form

$$\mathbf{U} = \begin{pmatrix} \rho \\ \rho u \\ \rho v \\ \rho w \\ \rho E \end{pmatrix}, \qquad \mathbf{F}(\mathbf{U}) = \begin{pmatrix} \rho u \\ \rho u^2 + p \\ \rho u v \\ \rho u w \\ \rho u H \end{pmatrix},$$

$$\mathbf{G}(\mathbf{U}) = \begin{pmatrix} \rho v \\ \rho u v \\ \rho v^2 + p \\ \rho v w \\ \rho v H \end{pmatrix}, \qquad \mathbf{H}(\mathbf{U}) = \begin{pmatrix} \rho w \\ \rho u w \\ \rho v w \\ \rho w^2 + p \\ \rho w H \end{pmatrix}.$$

# Euler equations

$$\frac{\partial}{\partial t}\int\limits_{V_i} \mathrm{U}^s \, \mathrm{d}V + \int\limits_{V_i} \boldsymbol{\nabla}\cdot\boldsymbol{\mathfrak{F}}^s \, \mathrm{d}V = 0$$

For finite-volume scheme, we work with integral form

Domain of interest is divided into small control volumes $V_i$

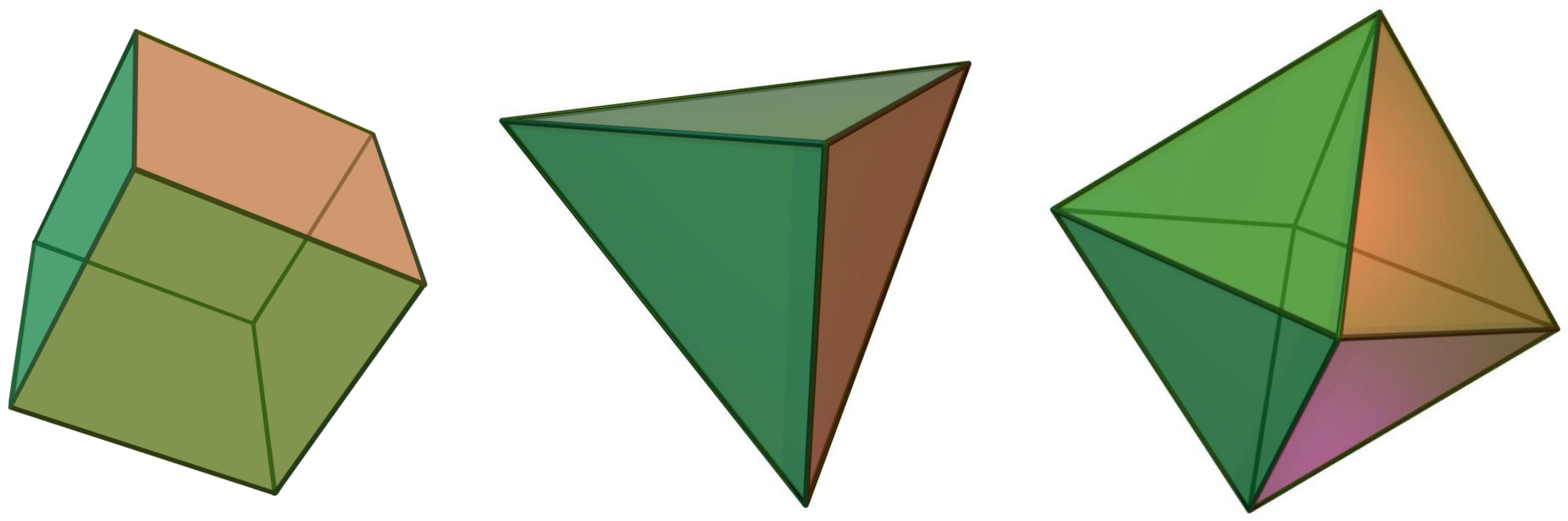

# Grid in astrophysics

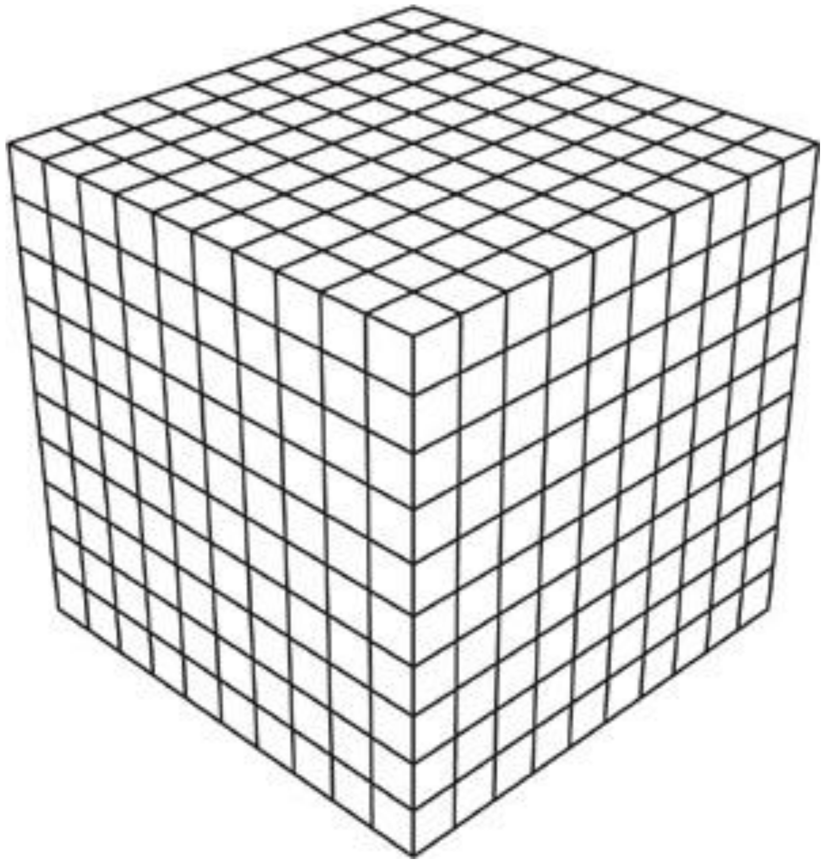

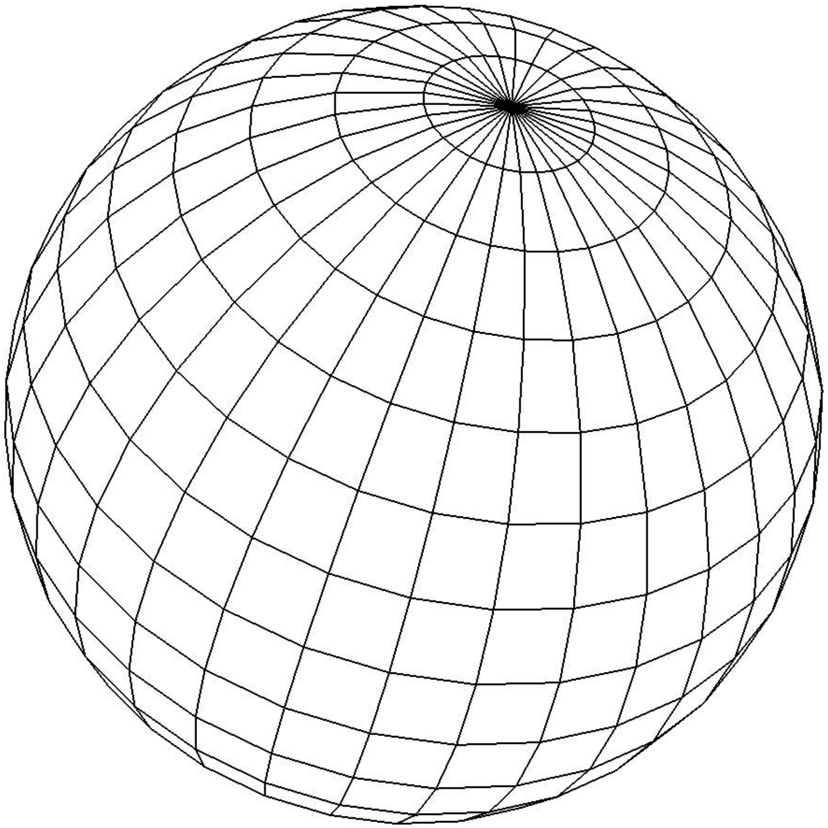

http://http.developer.nvidia.com/GPUGems3/elementLinks/22fig03.jpg

# Spherical polar grid

Singularities at poles and origin

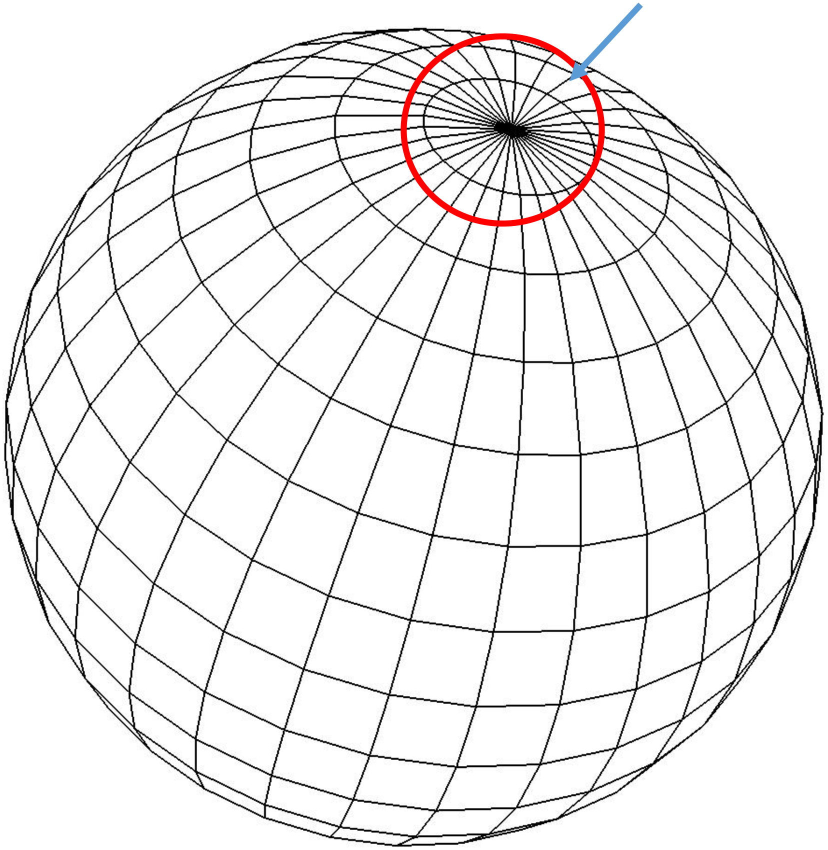

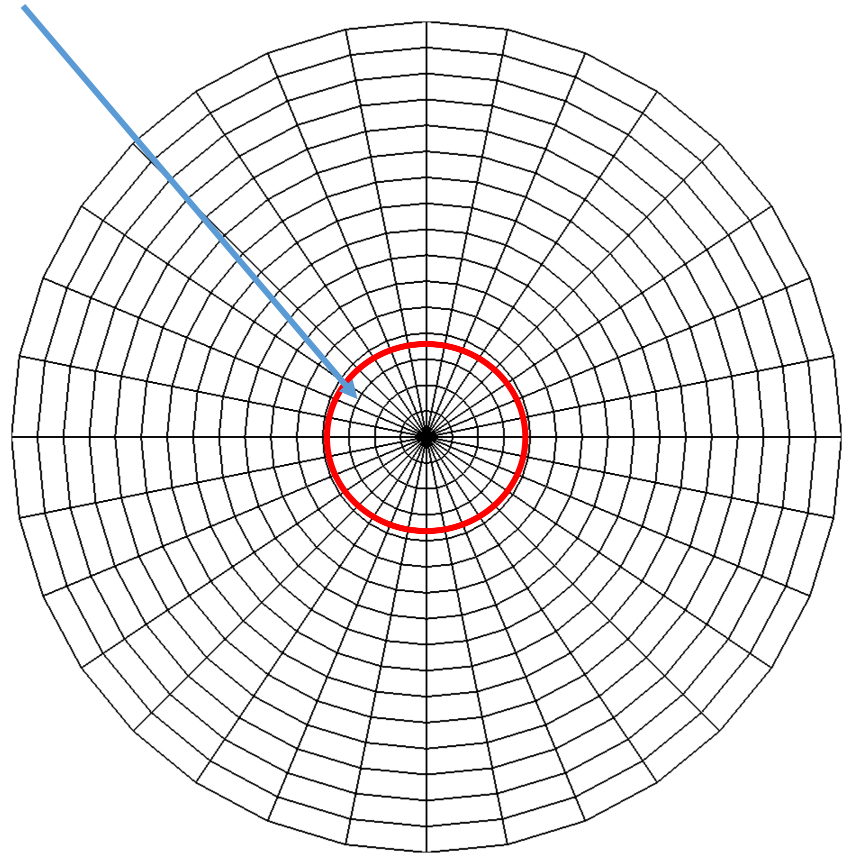

Time steps severely limited by CFL condition $$C = \Delta t \sum_{i=1}^{n} \frac{u_{x_i}}{\Delta x_i} \leq C_{\max}.$$

# Yin-Yang grid Kageyama&Sato (2004)

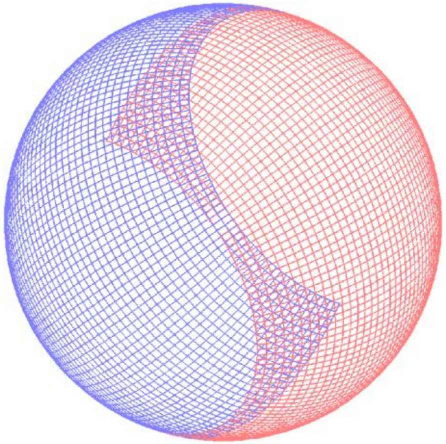

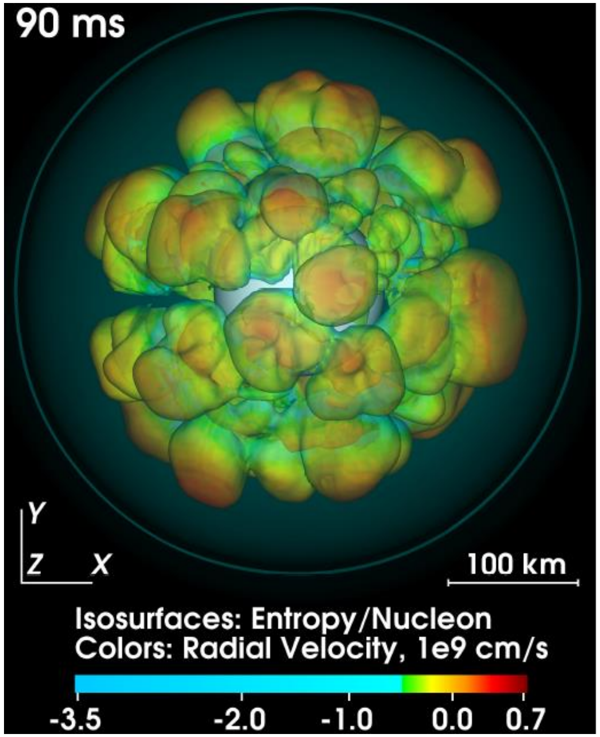


## Pole-problem solved

e.g., Melson et al. (2015)

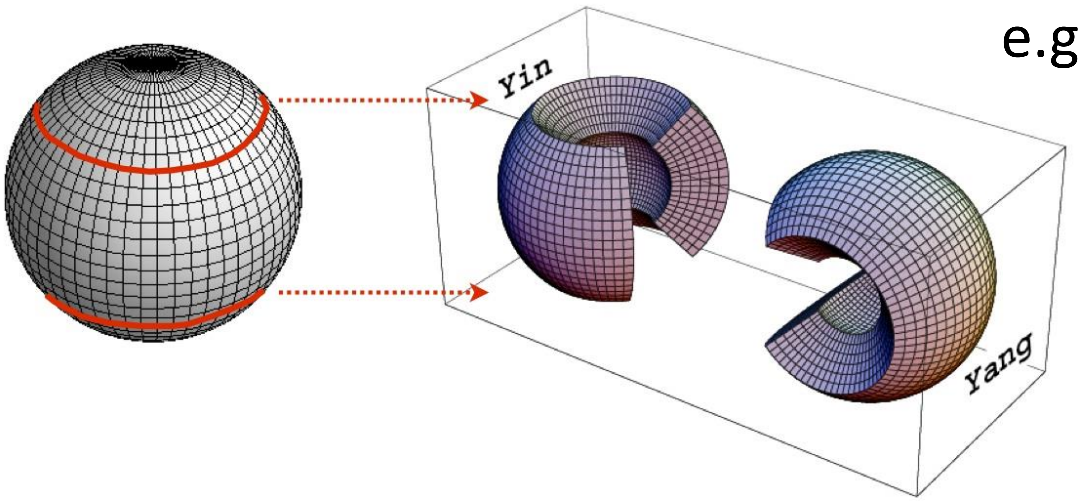


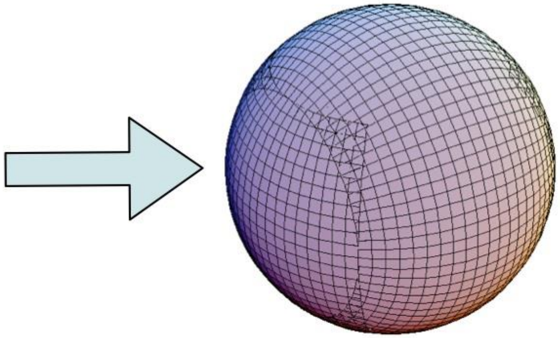

## But, singularity at the origin still remains

# Method

# Three main references

## A HIGH-ORDER FINITE-VOLUME METHOD FOR CONSERVATION LAWS ON LOCALLY REFINED GRIDS

PETER MCCORQUODALE AND PHILLIP COLELLA

## High-order, finite-volume methods in mapped coordinates

P. Colella [a,1], M.R. Dorr [b,2], J.A.F. Hittinger [b,*,2], D.F. Martin [a,1]

[a] *Applied Numerical Algorithms Group, Lawrence Berkeley National Laboratory, One Cyclotron Road Mail Stop 50A-1148, Berkeley, CA 94720, United States*
[b] *Center for Applied Scientific Computing, Lawrence Livermore National Laboratory, 7000 East Avenue L-561, Livermore, CA 94550, United States*

## A Freestream-Preserving High-Order Finite-Volume Method for Mapped Grids with Adaptive-Mesh Refinement

S. Guzik, P. McCorquodale , P. Colella

December 19, 2011

# Apsara: A multidimensional unsplit fourth-order explicit Eulerian hydrodynamics code for arbitrary curvilinear grids

A. Wongwathanarat, H. Grimm-Strele, and E. Müller

(figure from wikipedia)

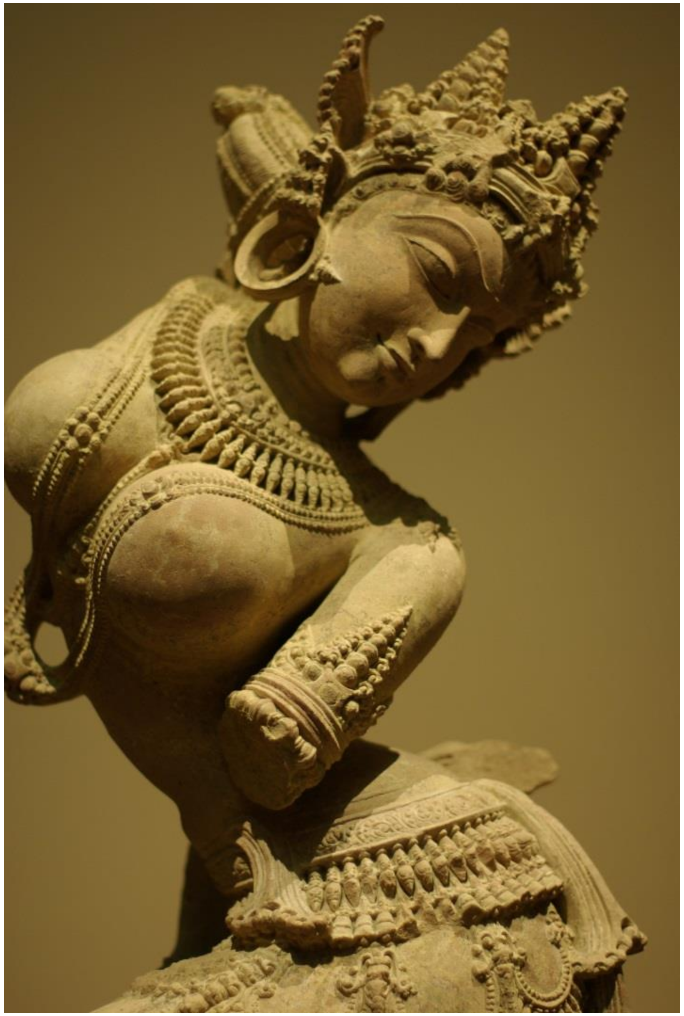

An Apsara is a female spirit of the clouds and water in Hindu mythology.
Apsaras are said to be able to change their shape at will.

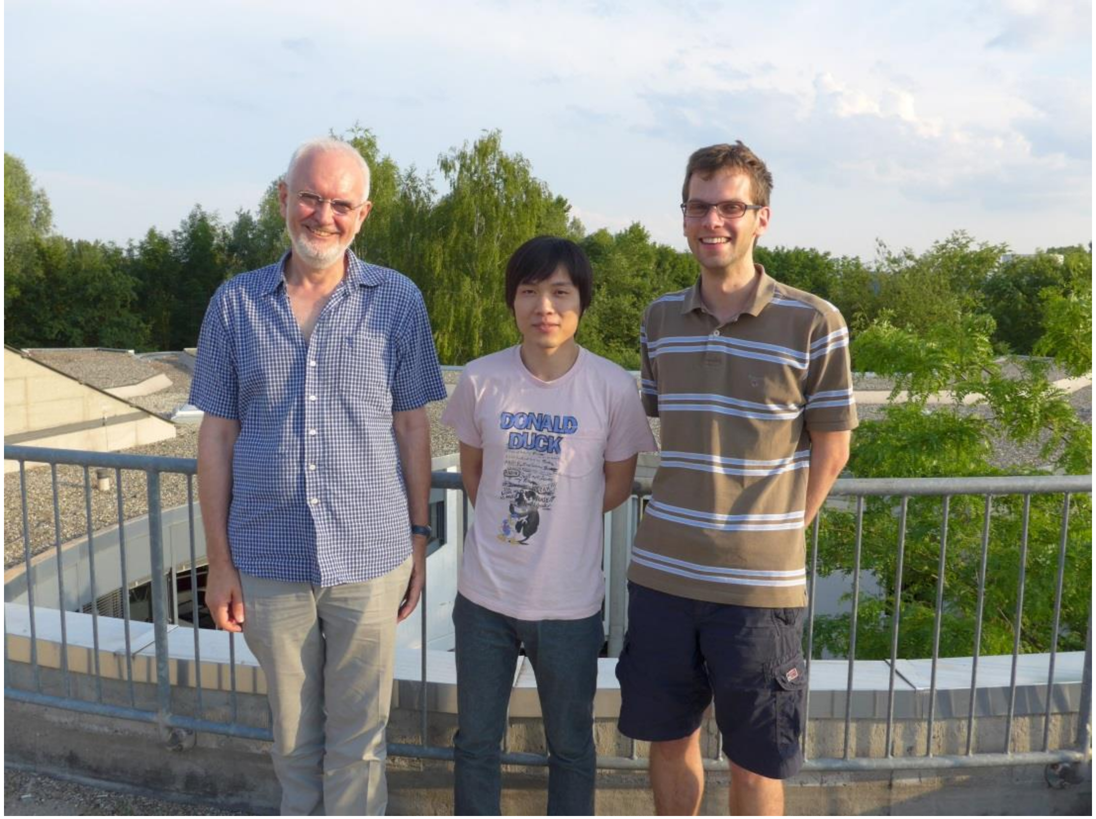

# Mapped grid technique

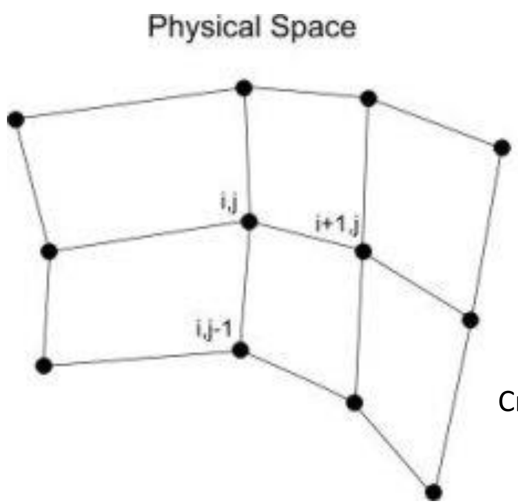


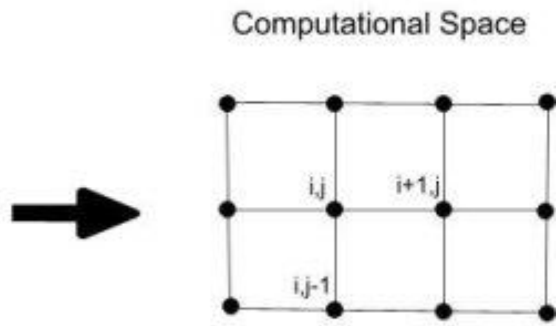


Credit: http://www.innovative-cfd.com/cfd-grid.html

Non-uniform grid in physical space is mapped to equidistant Cartesian grid in computational space

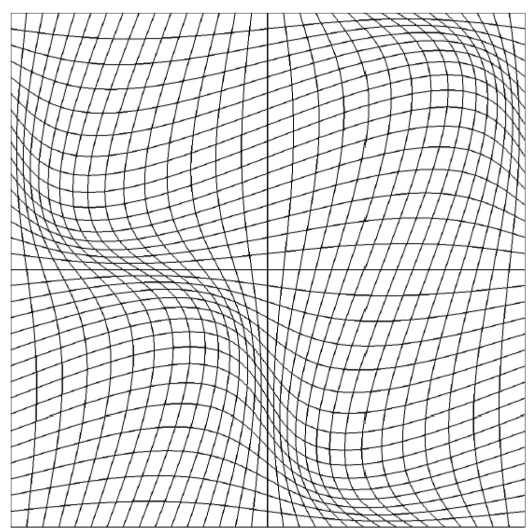

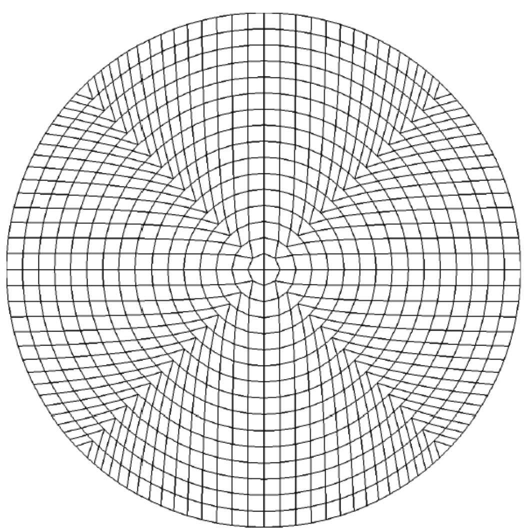

# Mapped grid technique

$$\frac{\partial}{\partial t}\int_{V_i} \mathrm{U}^s \,\mathrm{d}V + \int_{V_i} \boldsymbol{\nabla}\cdot\boldsymbol{\mathfrak{F}}^s \,\mathrm{d}V = 0 \Longrightarrow \frac{\partial}{\partial t}\int_{\Omega_i} J\mathrm{U}^s \,\mathrm{d}\Omega + \int_{\Omega_i} \boldsymbol{\nabla}_\xi\cdot(\mathbf{N}\boldsymbol{\mathfrak{F}}^s)\,\mathrm{d}\Omega = 0$$

Define one-to-one mapping function

$$\mathbf{M}(\xi) = \mathbf{x},\ \ \mathbf{M}:\mathbb{R}^3 \to \mathbb{R}^3.$$

$$\frac{\partial}{\partial t}\int_{\Omega_i} J\mathrm{U}^s \,\mathrm{d}\Omega + \int_{\partial\Omega_i} \mathbf{N}\boldsymbol{\mathfrak{F}}^s\cdot\,\mathrm{d}\mathbf{A}_\xi = 0.$$

$$J = \left|\frac{\partial(x,y,z)}{\partial(\xi,\eta,\zeta)}\right|$$

$$\mathbf{N} = \begin{pmatrix} \left|\frac{\partial(y,z)}{\partial(\eta,\zeta)}\right| & \left|\frac{\partial(z,x)}{\partial(\eta,\zeta)}\right| & \left|\frac{\partial(x,y)}{\partial(\eta,\zeta)}\right| \\ \left|\frac{\partial(y,z)}{\partial(\zeta,\xi)}\right| & \left|\frac{\partial(z,x)}{\partial(\zeta,\xi)}\right| & \left|\frac{\partial(x,y)}{\partial(\zeta,\xi)}\right| \\ \left|\frac{\partial(y,z)}{\partial(\xi,\eta)}\right| & \left|\frac{\partial(z,x)}{\partial(\xi,\eta)}\right| & \left|\frac{\partial(x,y)}{\partial(\xi,\eta)}\right| \end{pmatrix}.$$

# High-order mapped grid technique

$$\frac{\partial}{\partial t}\int_{\Omega_i} J\mathrm{U}^s\,\mathrm{d}\Omega + \int_{\partial\Omega_i} \mathbf{N}\mathfrak{F}^s\cdot\mathrm{d}\mathbf{A}_\xi = 0.$$

Approximate the volume and face integrals to high-order using Taylor expansions

$$\frac{\partial}{\partial t}\langle J\mathrm{U}^s\rangle_{\boldsymbol{i}} + \sum_{d=1}^{3}\left(\langle\mathbf{N}_d\mathfrak{F}^s\rangle_{\boldsymbol{i}+\frac{1}{2}\boldsymbol{e}^d} - \langle\mathbf{N}_d\mathfrak{F}^s\rangle_{\boldsymbol{i}-\frac{1}{2}\boldsymbol{e}^d}\right) = 0$$

$$\langle f\rangle_{\boldsymbol{i}} = f_{\boldsymbol{i}} + \frac{h^2}{24}\nabla_\xi^2 f$$

4th order cell average

$$\langle f\rangle_{\boldsymbol{i}\pm\frac{1}{2}\boldsymbol{e}^d} = f_{\boldsymbol{i}\pm\frac{1}{2}\boldsymbol{e}^d} + \frac{h^2}{24}\nabla_{\xi,\perp}^2 f$$

4th order face average

# High-order mapped grid technique

$$\frac{\partial}{\partial t}\langle J\mathrm{U}^s\rangle_i + \sum_{d=1}^{3}\left(\langle \mathbf{N}_d \boldsymbol{\mathfrak{F}}^s\rangle_{i+\frac{1}{2}e^d} - \langle \mathbf{N}_d \boldsymbol{\mathfrak{F}}^s\rangle_{i-\frac{1}{2}e^d}\right) = 0$$

## Product of two functions

$$\langle fg\rangle_i = \langle f\rangle_i\langle g\rangle_i + \frac{h^2}{12}\sum_{d=1}^{3}\frac{\partial f}{\partial \xi_d}\frac{\partial g}{\partial \xi_d}.$$

Use RK4 for time integration

Similarly, for face averages use only transverse gradients here

$$\frac{\Delta t}{h}\max_i\left(\sum_{d=1}^{3} J^{-1}(|\mathbf{N}\mathbf{v}\cdot \boldsymbol{e}^d| + c_s|(\mathbf{N}_d)^T|)\right) \lessapprox 1.3925,$$

# High-order mapped grid technique

How to calculate <N>??

We need to be very careful here -->
Freestream preservation

Consider an initial condition where
rho=p=const. and u=v=w=0

$$\sum_{\pm=+,-} \sum_{d=1}^{3} \pm \langle N_d^c \rangle_{\boldsymbol{i}\pm\frac{1}{2}\boldsymbol{e}^d} = 0.$$

# High-order mapped grid technique

How to calculate fluxes $\langle F \rangle$??

Non-linear conversion

$\langle JU \rangle_i \dashrightarrow \langle U \rangle_i \dashrightarrow U_i \dashrightarrow W_i \dashrightarrow \langle W \rangle_i$

then, reconstruct ---> solve Riemann problem ---> get new $\langle W \rangle_{i+1/2}$

$\langle W \rangle_{i+1/2} \dashrightarrow W_{i+1/2} \dashrightarrow F_{i+1/2} \dashrightarrow \langle F \rangle_{i+1/2}$

# Testing the code

## Linear advection

$$\rho(r) = 1 + e^{-256(r-\frac{1}{2})^2}$$

u=1

t=10

1D

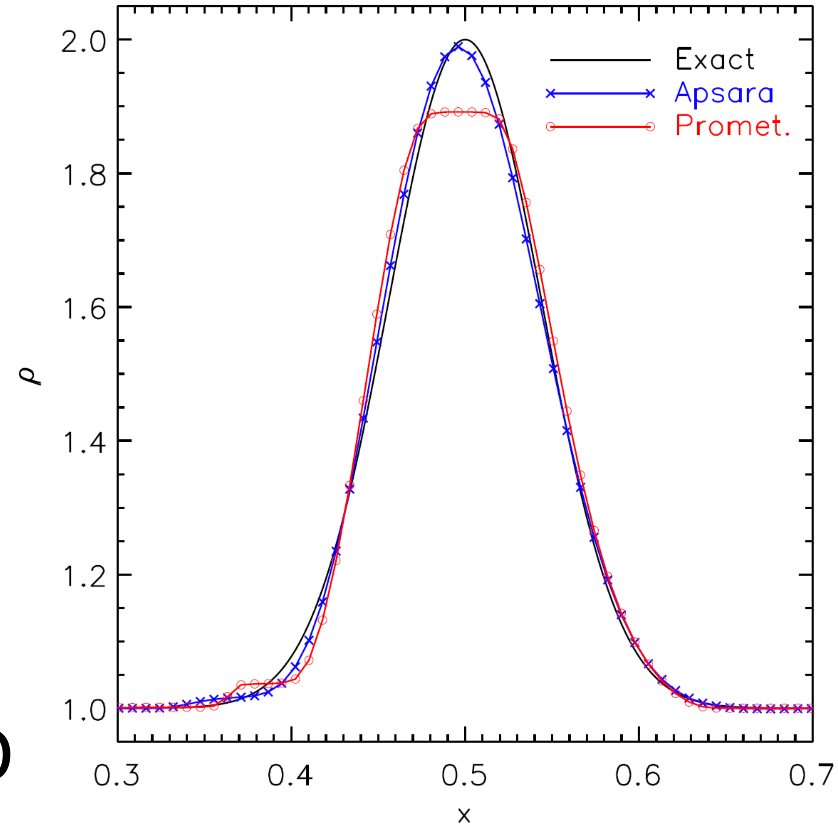


| Grid size | APSARA | | | | PROMETHEUS | | | |
|---|---|---|---|---|---|---|---|---|
| | $L_1$ | Rate | $L_\infty$ | Rate | $L_1$ | Rate | $L_\infty$ | Rate |
| 32 | 6.13E-02 | - | 3.92E-01 | - | 6.02E-02 | - | 4.24E-01 | - |
| 64 | 2.04E-02 | 1.59 | 1.65E-01 | 1.24 | 2.65E-02 | 1.18 | 2.40E-01 | 0.82 |
| 128 | 4.75E-03 | 2.10 | 4.02E-02 | 2.04 | 9.60E-03 | 1.47 | 1.04E-01 | 1.20 |
| 256 | 2.99E-04 | 3.99 | 2.67E-03 | 3.91 | 2.05E-03 | 2.23 | 3.29E-02 | 1.67 |
| 512 | 1.88E-05 | 3.99 | 1.66E-04 | 4.01 | 4.33E-04 | 2.24 | 1.01E-02 | 1.70 |
| 1024 | 1.18E-06 | 4.00 | 1.04E-05 | 4.00 | 6.25E-05 | 2.79 | 3.08E-03 | 1.71 |

# Testing the code

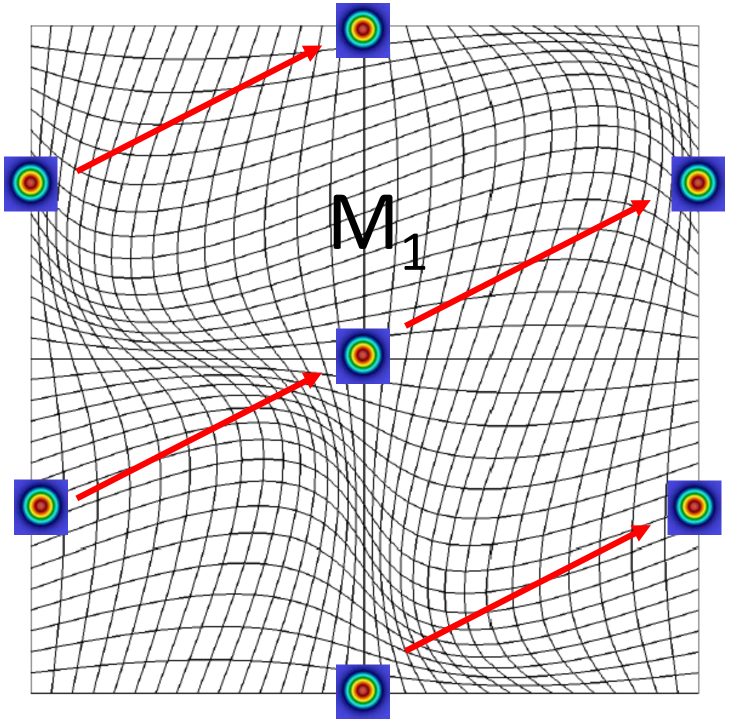


$$\rho(r) = 1 + e^{-256(r-\frac{1}{2})^2}$$

u=1, v=0.5

t=2

2D

| Grid size | Apsara M0 $L_1$ | Rate | $L_\infty$ | Rate | Apsara M1 $L_1$ | Rate | $L_\infty$ | Rate | Prometheus $L_1$ | Rate | $L_\infty$ | Rate |
|---|---|---|---|---|---|---|---|---|---|---|---|---|
| $32^2$ | 4.74E-03 | - | 3.36E-01 | - | 7.08E-03 | - | 4.39E-01 | - | 5.12E-03 | - | 4.34E-01 | - |
| $64^2$ | 1.27E-03 | 1.90 | 8.02E-02 | 2.07 | 1.84E-03 | 1.95 | 1.49E-01 | 1.56 | 2.58E-03 | 0.99 | 2.21E-01 | 0.97 |
| $128^2$ | 1.16E-04 | 3.45 | 1.08E-02 | 2.89 | 2.89E-04 | 2.67 | 2.73E-02 | 2.45 | 8.15E-04 | 1.66 | 1.46E-01 | 0.60 |
| $256^2$ | 7.39E-06 | 3.97 | 6.84E-04 | 3.98 | 1.90E-05 | 3.93 | 1.96E-03 | 3.80 | 1.51E-04 | 2.43 | 3.36E-02 | 2.12 |
| $512^2$ | 4.64E-07 | 3.99 | 4.30E-05 | 3.99 | 1.19E-06 | 3.99 | 1.23E-04 | 3.99 | 3.09E-05 | 2.29 | 1.09E-02 | 1.62 |

# Testing the code

## Linear acoustic wave

$\rho_0 = 1$ and $p_0 = \frac{3}{5}$

$$\delta \mathbf{U} = A \sin(2\pi x) \cdot (1, -1, 1, 1, 1.5)^T$$

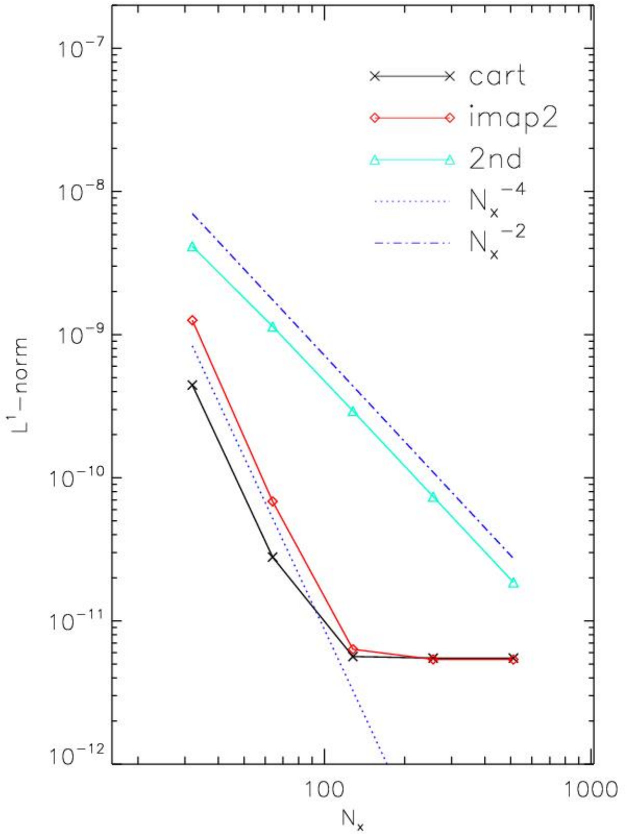


| Grid size | fourth-order scheme | | second-order scheme | |
|---|---|---|---|---|
| | $\epsilon$ | Rate | $\epsilon$ | Rate |
| 32 | 2.39E-09 | - | | |
| 64 | 1.06E-10 | 4.50 | | |
| 128 | 7.56E-12 | 3.80 | | |
| 256 | 5.51E-12 | 0.46 | | |
| 512 | 5.50E-12 | 0.00 | | |
| 1024 | 5.50E-12 | 0.00 | | |
| $32^2$ | 1.36E-09 | - | 4.85E-09 | - |
| $64^2$ | 7.19E-11 | 4.24 | 1.19E-09 | 2.02 |
| $128^2$ | 6.59E-12 | 3.45 | 2.98E-10 | 2.00 |
| $256^2$ | 5.50E-12 | 0.26 | 7.46E-11 | 2.00 |
| $512^2$ | 5.50E-12 | 0.00 | 1.91E-11 | 1.96 |
| $1024^2$ | 5.50E-12 | 0.00 | 6.96E-12 | 1.46 |
| $32^3$ | 8.68E-10 | - | 4.34E-09 | - |
| $64^3$ | 5.03E-11 | 4.11 | 1.08E-09 | 2.00 |
| $128^3$ | 5.99E-12 | 3.07 | 2.72E-10 | 1.99 |
| $256^3$ | 5.96E-12 | 0.01 | 6.82E-11 | 1.99 |

Non-linear terms intervene

# Testing the code

## Linear acoustic wave

$\rho_0 = 1$ and $p_0 = \frac{3}{5}$

$\delta \mathbf{U} = A \sin(2\pi x) \cdot (1, -1, 1, 1, 1.5)^T$

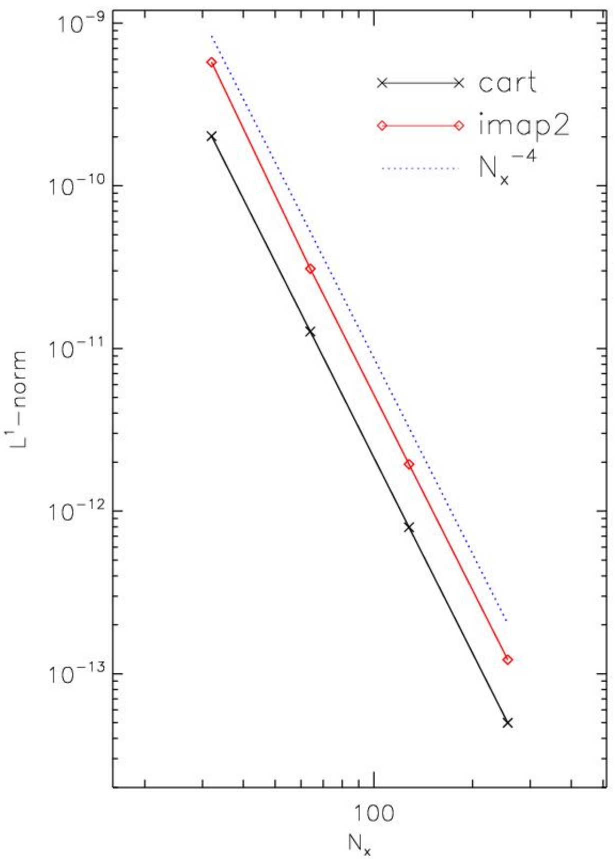


| Grid size | fourth-order scheme | | second-order scheme | |
|---|---|---|---|---|
| Coarse : Fine | $L_1(\Delta\rho)$ | Rate | $L_1(\Delta\rho)$ | Rate |
| 32 : 64 | 1.12E-09 | - | | |
| 64 : 128 | 4.80E-11 | 4.55 | | |
| 128 : 256 | 3.02E-12 | 3.99 | | |
| 256 : 512 | 1.89E-13 | 4.00 | | |
| 512 : 1024 | 1.20E-14 | 3.97 | | |
| $32^2 : 64^2$ | 6.26E-10 | - | 1.82E-09 | - |
| $64^2 : 128^2$ | 3.28E-11 | 4.26 | 4.39E-10 | 2.05 |
| $128^2 : 256^2$ | 2.07E-12 | 3.99 | 1.10E-10 | 2.00 |
| $256^2 : 512^2$ | 1.31E-13 | 3.98 | 2.74E-11 | 2.00 |
| $512^2 : 1024^2$ | 9.60E-15 | 3.77 | 6.85E-12 | 2.00 |
| $32^3 : 64^3$ | 3.95E-10 | - | 1.71E-09 | - |
| $64^3 : 128^3$ | 2.28E-11 | 4.11 | 4.31E-10 | 1.99 |
| $128^3 : 256^3$ | 1.45E-12 | 3.97 | 1.09E-10 | 1.99 |

## Self convergence

# *Gresho vortex*

$$\frac{u_\phi(r)}{0.4\pi} = \begin{cases} 5r & ;\ 0 \leq r < 0.2, \\ 2 - 5r & ;\ 0.2 \leq r < 0.4, \\ 0 & ;\ 0.4 \leq r. \end{cases}$$

$$p(r) = \begin{cases} p_0 + \frac{25}{2} r^2 & ;\ 0 \leq r < 0.2, \\ p_0 + \frac{25}{2} r^2 + 4(1 - 5r - \ln 0.2 + \ln r) & ;\ 0.2 \leq r < 0.4, \\ p_0 - 2 + 4 \ln 2 & ;\ 0.4 \leq r, \end{cases}$$

$$p_0 = \frac{(0.4\pi)^2}{\gamma M_{\max}^2} - \frac{1}{2}$$

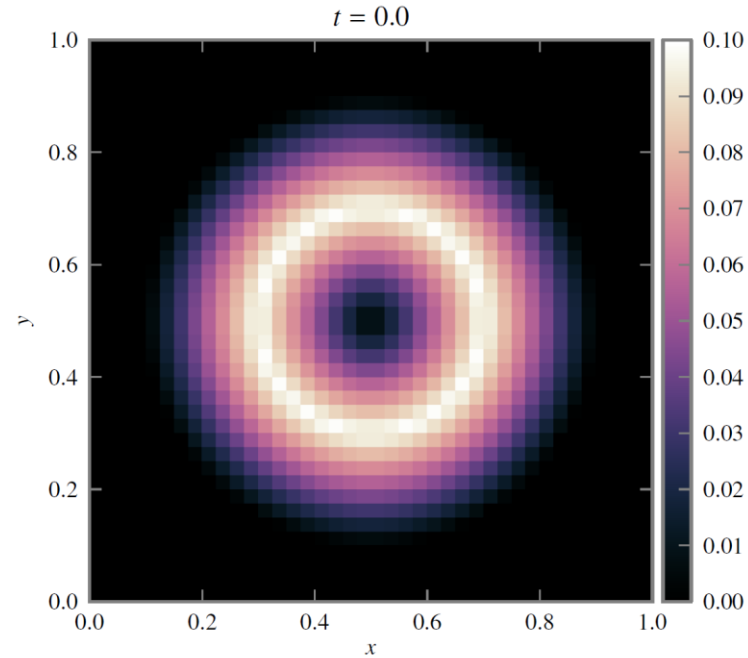


**A new numerical solver for flows at various Mach numbers**


F. Miczek[1], F. K. Röpke[2], and P. V. F. Edelmann[2,1]

[1] Max-Planck-Institut für Astrophysik, Karl-Schwarzschild-Str. 1, D-85741 Garching, Germany
e-mail: `fab@miczek.de`
[2] Institut für Theoretische Physik und Astrophysik, Universität Würzburg, Emil-Fischer-Str. 31, D-97074 Würzburg, Germany

# *Gresho vortex*

## Failure of Roe type flux

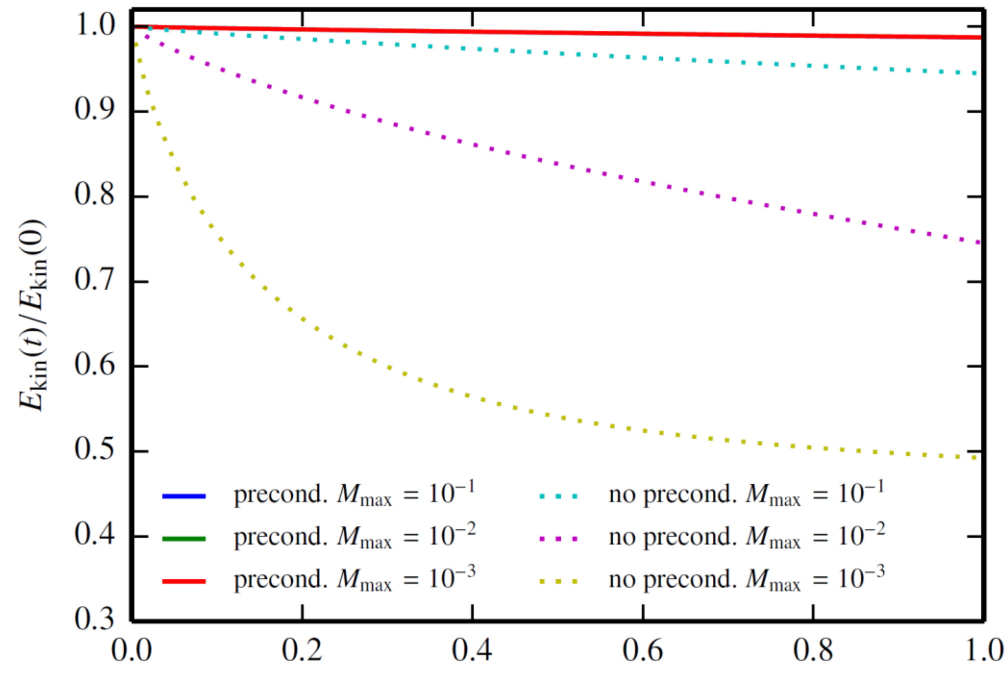


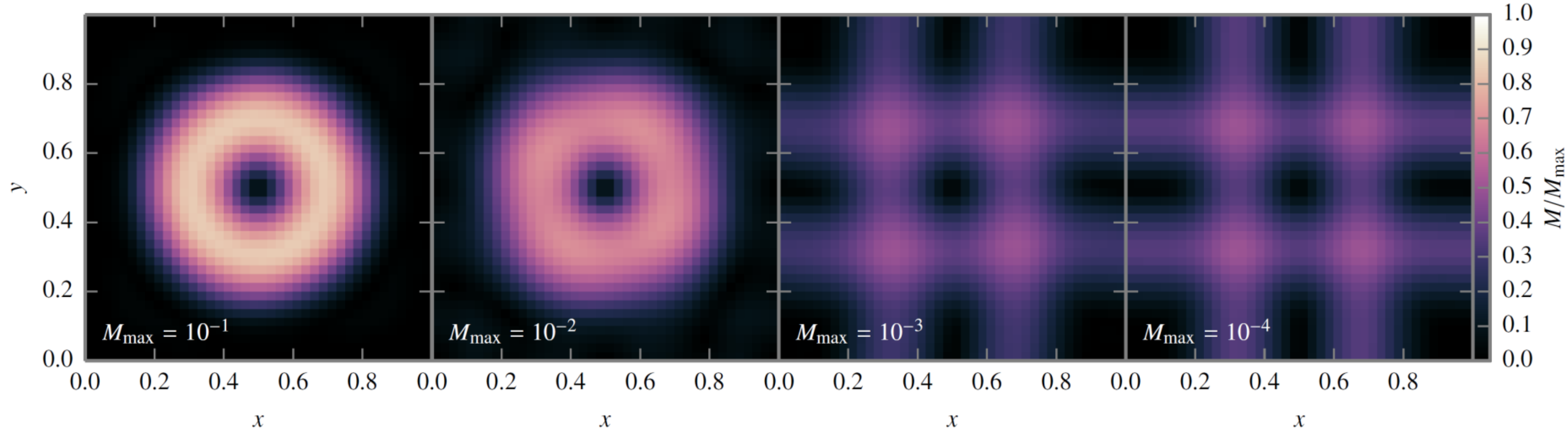


**Fig. 4.** Gresho vortex problem advanced to $t = 1.0$ with the Roe flux discretization scheme for different maximum Mach numbers $M_{\mathrm{max}}$ in the setup, as indicated in the plots. Color coded is the Mach number relative to the respective $M_{\mathrm{max}}$.

*Gresho vortex*

APSARA can capture low-mach number flows better

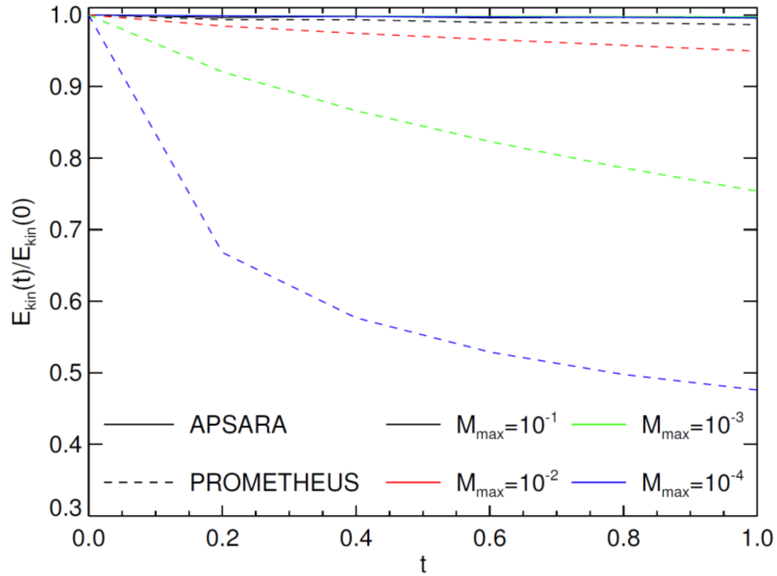


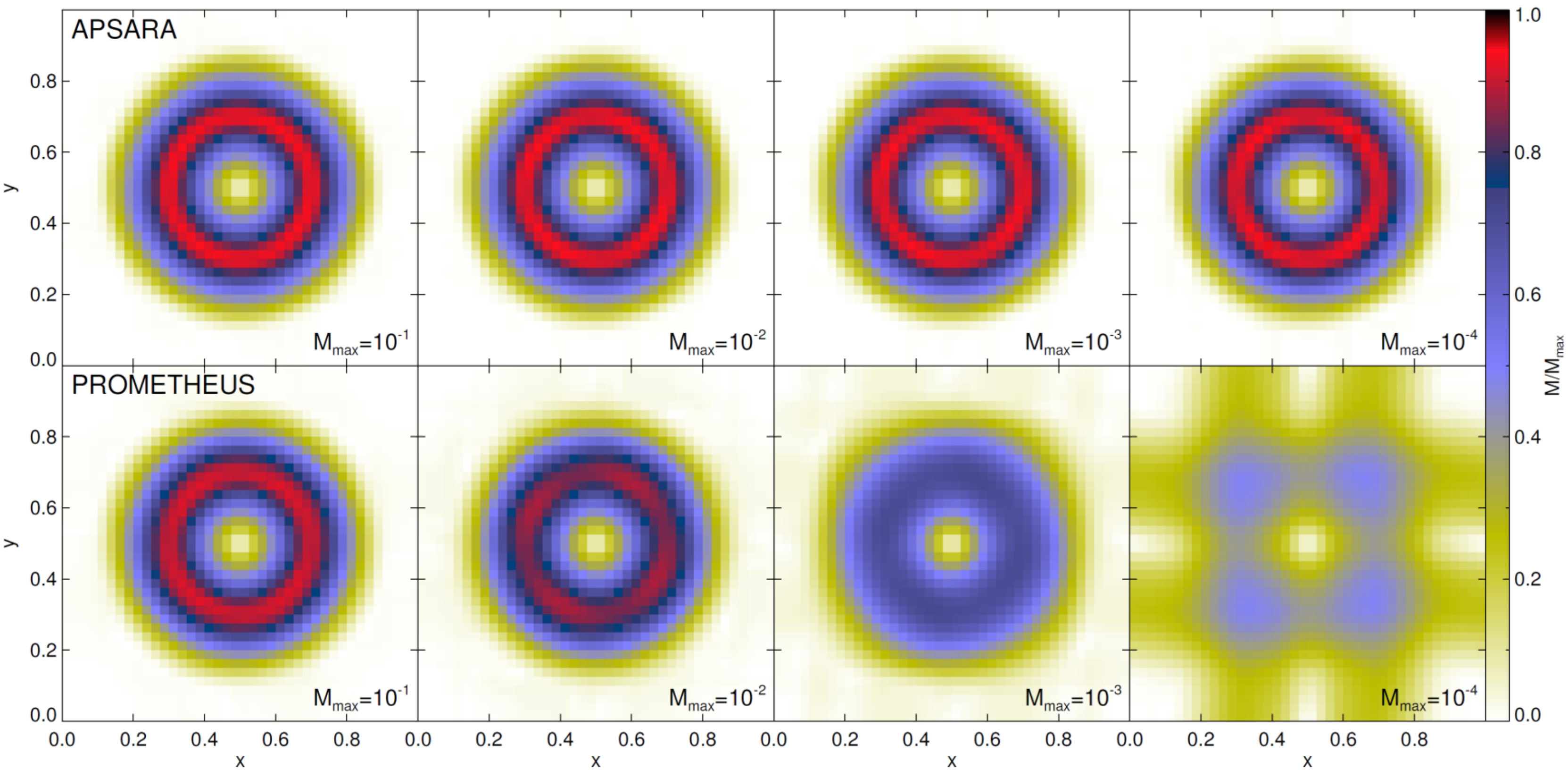

# Testing the code

## Non-linear vortex advection

$$\rho_0 = p_0 = T_0 = 1, \qquad u_0 = v_0 = 1.$$

$$(\delta u, \delta v) = \frac{\epsilon}{2\pi} e^{\frac{1-r^2}{2}} (-\bar{y}, \bar{x}),$$

$$\delta T = -\frac{(\gamma - 1)\epsilon^2}{8\gamma\pi^2} e^{\frac{1-r^2}{2}},$$

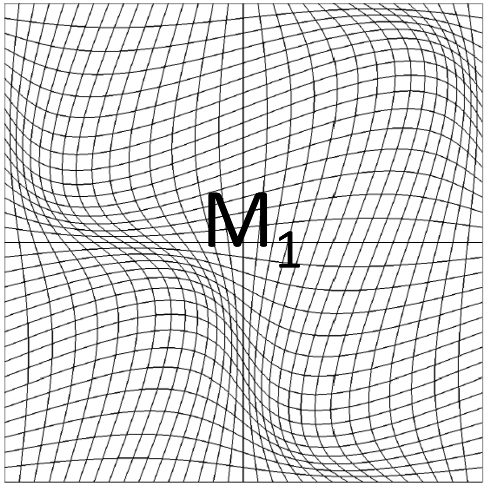


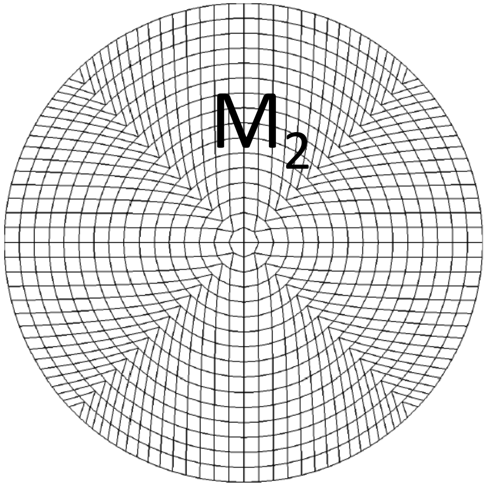


| Grid size | $\mathbf{M_1}$ | | | | $\mathbf{M_2}$ | | | |
|---|---|---|---|---|---|---|---|---|
| | $L_1$ | Rate | $L_\infty$ | Rate | $L_1$ | Rate | $L_\infty$ | Rate |
| $32^2$ | 4.56E-01 | - | 9.22E-02 | - | 5.40E-01 | - | 9.06E-02 | - |
| $64^2$ | 4.89E-02 | 3.22 | 7.90E-03 | 3.54 | 1.39E-01 | 1.96 | 2.99E-02 | 1.60 |
| $128^2$ | 3.25E-03 | 3.91 | 4.77E-04 | 4.05 | 4.41E-02 | 1.66 | 1.54E-02 | 0.96 |
| $256^2$ | 2.08E-04 | 3.96 | 3.09E-05 | 3.95 | 1.48E-02 | 1.58 | 8.93E-03 | 0.79 |
| $512^2$ | 1.31E-05 | 3.99 | 1.95E-06 | 3.98 | 5.16E-03 | 1.52 | 4.15E-03 | 1.11 |
| $1024^2$ | 8.18E-07 | 4.00 | 1.23E-07 | 3.99 | 1.92E-03 | 1.42 | 2.13E-03 | 0.96 |

Non-smooth grid destroys convergence

# Single block circular domain

Low quality grid cells along diagonals

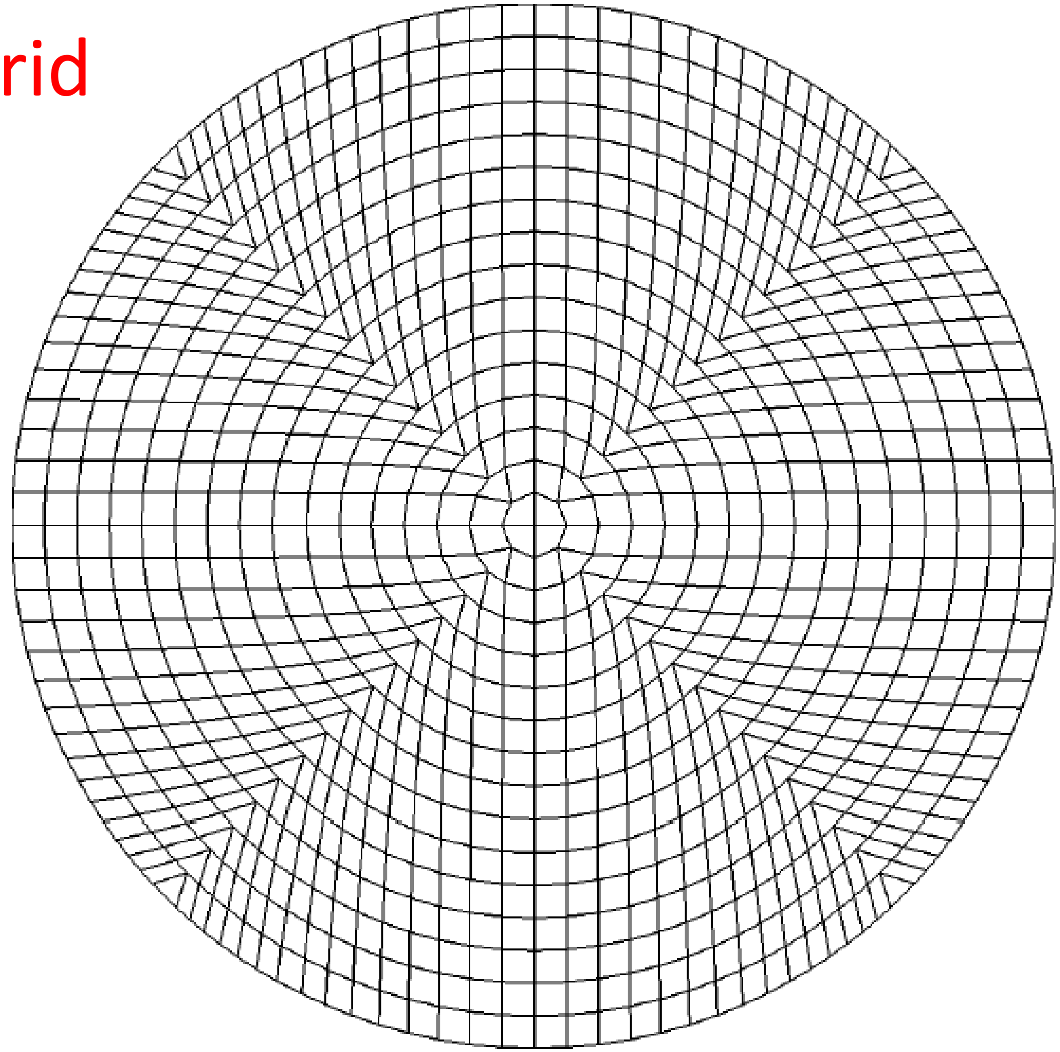

# Mapped multi-block grid

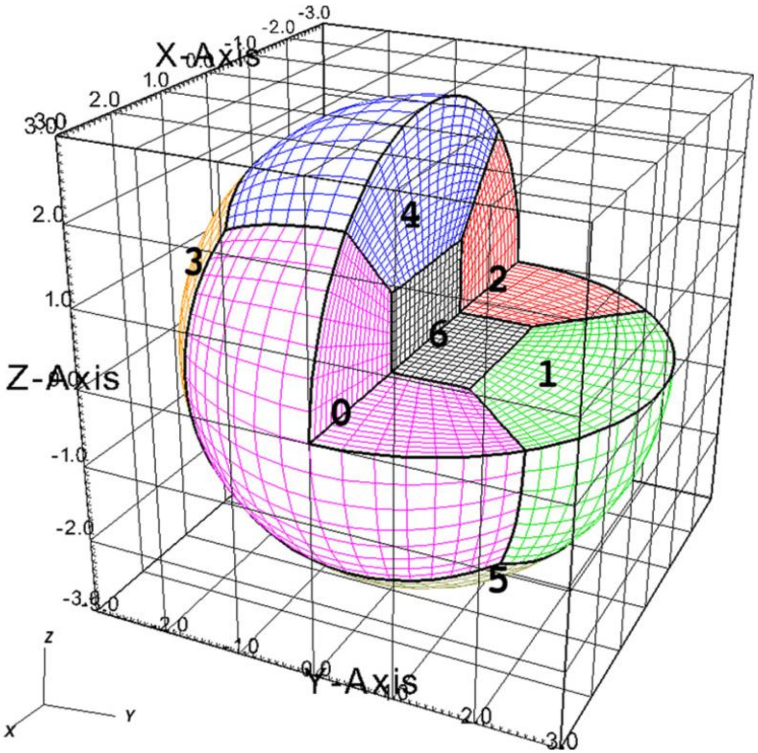


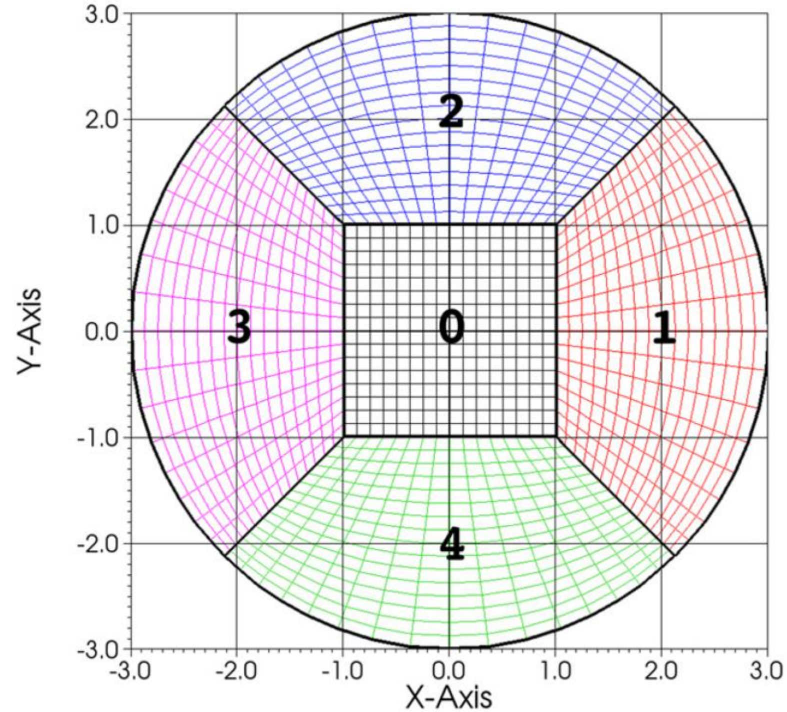


High-order finite-volume methods for hyperbolic conservation laws on mapped multiblock grids

P. McCorquodale [a,*], M.R. Dorr [b], J.A.F. Hittinger [b], P. Colella [a]

[a] Computational Research Division, Lawrence Berkeley National Laboratory, 1 Cyclotron Road, Mail Stop 50A1148, Berkeley, CA 94720, USA
[b] Center for Applied Scientific Computing, Lawrence Livermore National Laboratory, P.O. Box 808, L-561, Livermore, CA 94551-0808, USA

## First results

# Linear advection   Gaussian profile, u=1, v=0.5

t=2

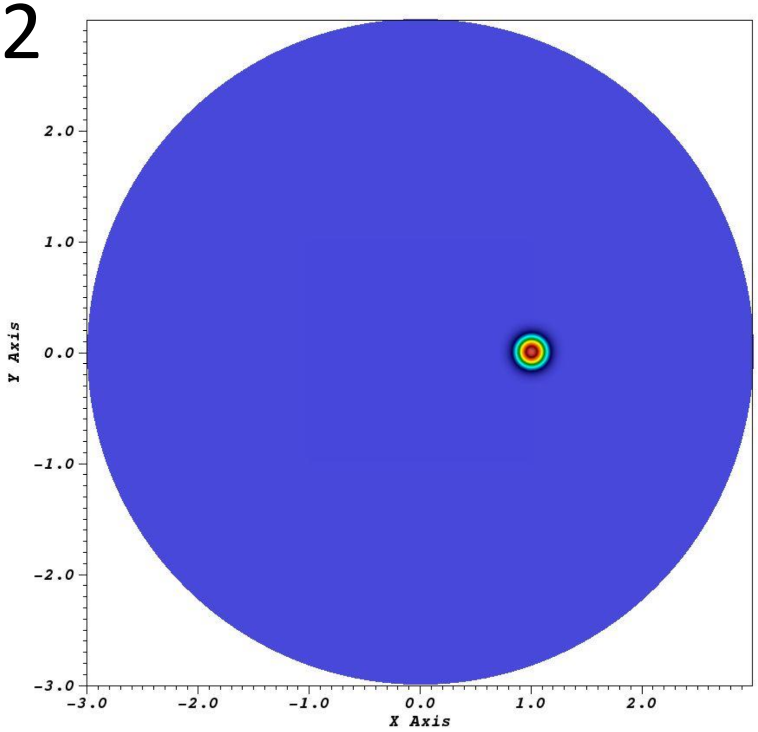


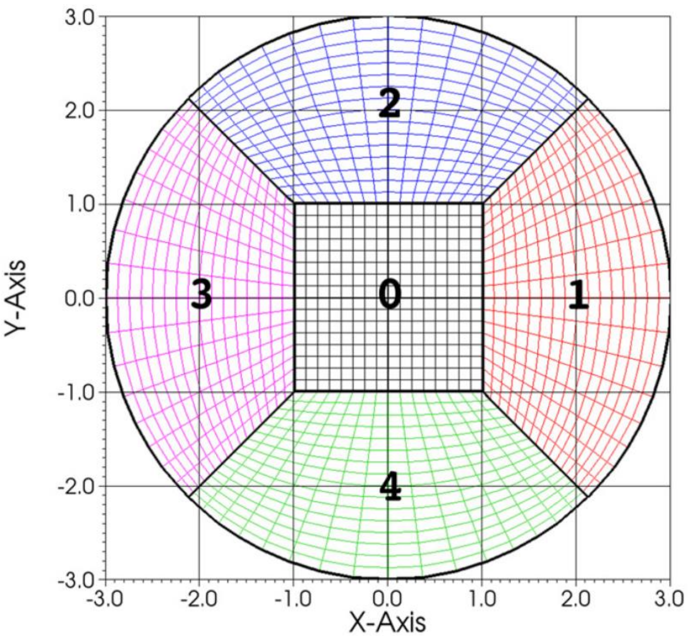


| | L1 | Rate | LM | Rate |
|---|---|---|---|---|
| 32 : | 1.38E-02 | 0.00E+00 | 2.63E-01 | 0.00E+00 |
| 64 : | 3.00E-03 | 2.20E+00 | 4.69E-02 | 2.49E+00 |
| 128 : | 2.29E-04 | 3.71E+00 | 5.38E-03 | 3.12E+00 |
| 256 : | 1.46E-05 | 3.97E+00 | 3.56E-04 | 3.92E+00 |
| 512 : | 9.23E-07 | 3.99E+00 | 2.25E-05 | 3.98E+00 |
| 1024: | 5.80E-08 | 3.99E+00 | 1.47E-06 | 3.94E+00 |
| 2048: | 3.65E-09 | 3.99E+00 | 9.77E-08 | 3.91E+00 |

$4^{th}$ order convergence achieved

# First results    Gaussian acoustic pulse

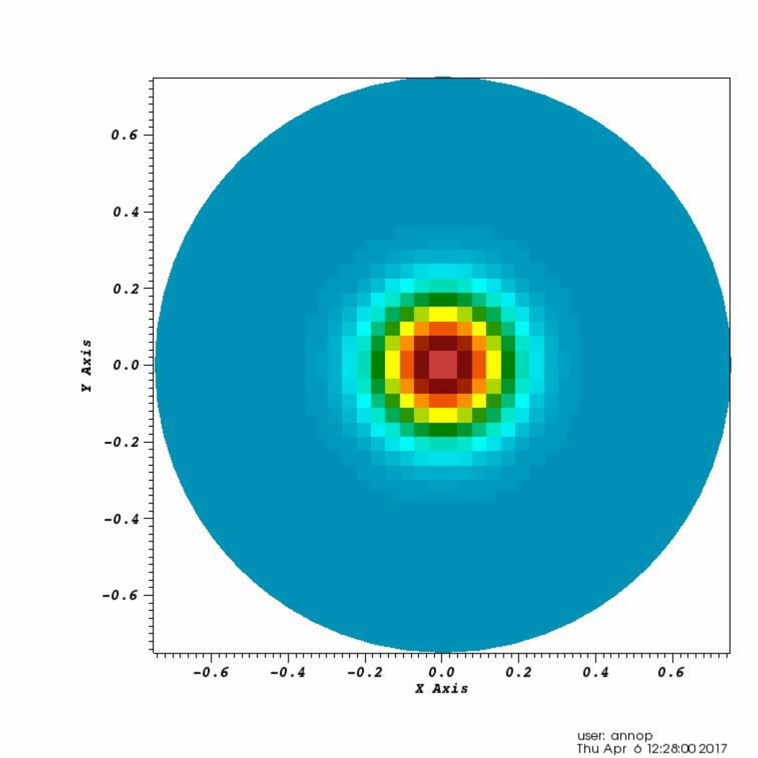


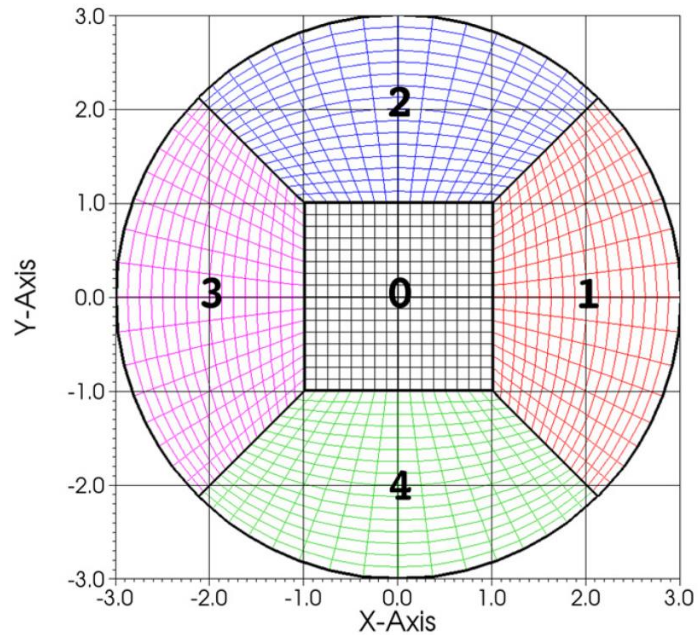


```
--- L^infty --------------------
                    DIFF        Rate
16/32      :   7.92E-04   0.00E+00
32/64      :   4.41E-05   4.17E+00
64/128     :   2.81E-06   3.97E+00
128/256    :   1.79E-07   3.98E+00
256/512    :   1.06E-08   4.08E+00
```

```
--- L^1------------------------
                    DIFF        Rate
16/32      :   1.01E-04   0.00E+00
32/64      :   7.20E-06   3.81E+00
64/128     :   4.74E-07   3.93E+00
128/256    :   3.01E-08   3.98E+00
256/512    :   1.89E-09   3.99E+00
```

## Conclusion

- Developed 4$^{th}$ order accurate hydrodynamic code APSARA

- test (smooth flow) problems show 4$^{th}$ order convergence
- better behavior for low Mach number flows

- Extension to multi-block grids in progress … first results looking good

## Outlook

- Flows with discontinuities (e.g., dissipation mechanisms for shocks, steepening of contact discontinuity)
- Multi-fluid advection

- Self-gravity

# Preliminary